Theoretical Study of Plasmonically Induced Transparency Effect in Arrays of Graphene-Based Double Disk Resonators

Gianni Portela[1] (ID), Victor Dmitriev[1] (ID), Cristiano Oliveira[1] (ID), Wagner Castro[2] (ID)
[1]Faculty of Electrical and Biomedical Engineering, Federal University of Pará, Belém, Brazil
gianni@ufpa.br,victor@ufpa.br,cboliveira@ufpa.br
[2]Cyberspace Institute, Federal Rural University of Amazônia, Belém, Brazil
wagner.ormanes@ufra.edu.br

Abstract— **In this paper, we consider coupled disk-shaped resonators separated by a thin dielectric substrate that can be used as frequency-tunable filters or as electromagnetic switches in the terahertz frequency band. The two disks are electromagnetically coupled and resonate with dipole plasmonic modes. By using a Temporal Coupled-Mode Theory based approach, we show how to analytically calculate the frequency response of such structures.The analytical results are in good agreement with those obtained from computational simulations based on the finite element method.**

Index Terms—filters, graphene, plasmonically induced transparency,temporal coupled-mode theory.

I. INTRODUCTION

Terahertz frequency range (THz) of the electromagnetic spectrum is attracting a lot of interest during the last years. Among the several applications that rely on the advantages of using terahertz radiation, the development of terahertz communications systems with high performance stands out [1], [2].

Several materials can be used on the project of new components for terahertz applications. In this context, graphene emerge as an interesting alternative. High rigidity, good thermal and electrical conductivity, presence of plasmon resonances, and dynamic control of its physical properties by electrostatic and magnetostatic fields are some of the outstanding features of its two-dimensional structure [3]-[6]. These features enable the use of graphene, for example, in the design of field effect transistors (FETs) [7], photodetectors [8], and antennas [9].

Besides, graphene-based resonators can be projected for operation at terahertz frequencies. They can be, for example, disk, ring, tape, square or cross shaped, and rely on the excitation of plasmon resonances. In the case where two graphene resonators are mutually coupled, one can verify, in the frequency response of the coupled system, a plasmonically induced transparency (PIT) band [5]. The PIT region is located between the resonance frequencies of the individual resonators and its main characteristic is the presence of transmission levels close to 100%.

Analytical methods can be used for the study of coupled resonators systems. Among them, Temporal Coupled-Mode Theory (TCMT) [10] is one of the most valuable, since it describes a given

Brazilian Microwave and Optoelectronics Society-SBMO
Brazilian Society of Electromagnetism-SBMag
received 4 Sept 2018; for review 6 Sept 2018; accepted 30 Nov 2018
© 2019 SBMO/SBMag
(cc) BY
ISSN 2179-1074

system in terms of the couplings that take place between its constitutive parts, like waveguides and resonators, and provides an easy way for the calculation of the frequency response of such structures.

These theoretical methods are very useful mainly because they allow the designer to quickly obtain several information of the system from a set of formulas. The knowledge obtained from theoretical analysis can provide, for example, a way to reduce the time spent on the realization of computational simulations or assembling experimental setups, speeding up the project of such components.

In this paper, we consider graphene-based double resonators consisting of two disk-shaped resonators located on opposite sides of a dielectric substrate. These structures can be used, for example, as switches or wavelength-selective filters in terahertz communication systems. In order to improve their performance, we have developed an analytical approach based on the application of Temporal Coupled-Mode Theory. This analytical model provides several insights that can be useful for tuning the quality factors of the coupled resonators and the bandwidth of the PIT region.

II. STRUCTURE AND DESIGN

In Fig. 1, we schematically show the unit cell of the array composed of two graphene disks with diameters $d = 32$ μm (disk 1) and $D = 60$ μm (disk 2) – see Appendix A for more details regarding the calculation of the disks diameters.
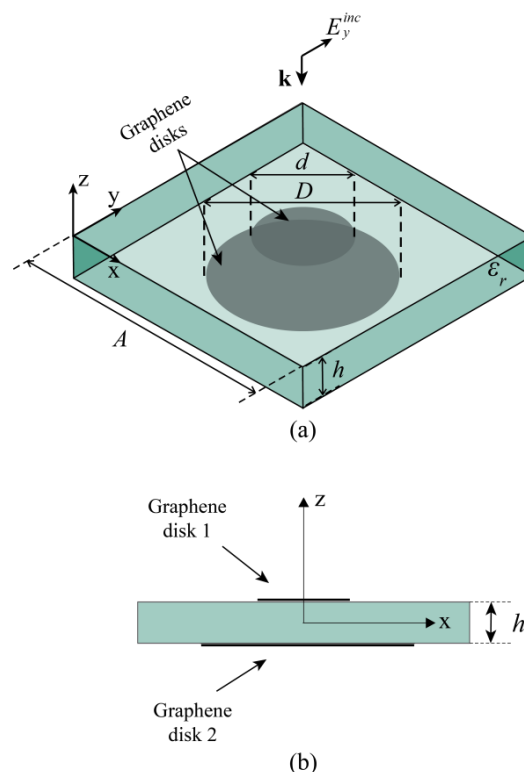

(a)

(b)

Fig.1. (a) Isometric view of the unit cell of the array (diameter d for the smaller disk and D for the larger one). The disks are separated by a dielectric substrate with thickness h. The incident TEM electromagnetic wave is polarized along y-axis. (b) Side view of the unit cell.

The resonator disks are placed on opposite sides of a dielectric substrate with unit cell size $A = 100$ μm, thickness $h = 10$ μm, relative permittivity $\varepsilon_r = 3.75$ and dielectric loss tangent $tan\delta = 0.0184$. In order to verify the influence of the dielectric substrate on the frequency response of the device, we
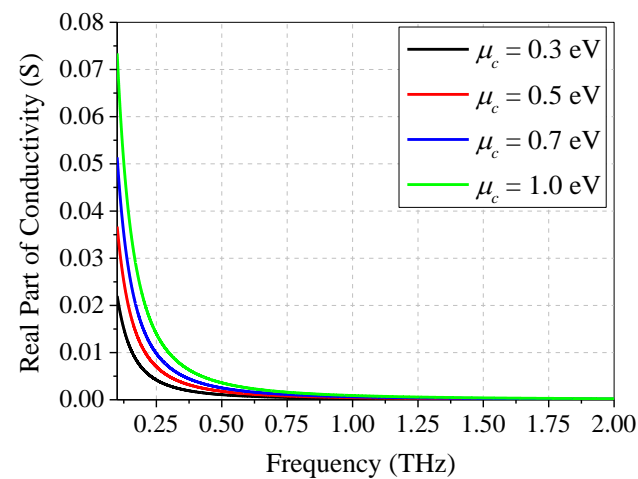
have also performed some computational simulations with the two disks suspended in air.

We have considered only the intra-band contributions for the calculation of graphene conductivity (σ_g) in this paper. The influence of inter-band transitions can be neglected in the considered operating frequency range, since the condition $\hbar\omega << 2\mu_c$ is satisfied [11]. Therefore, the following formula derived from Kubo formalism [6] can be used for the calculation of σ_g:
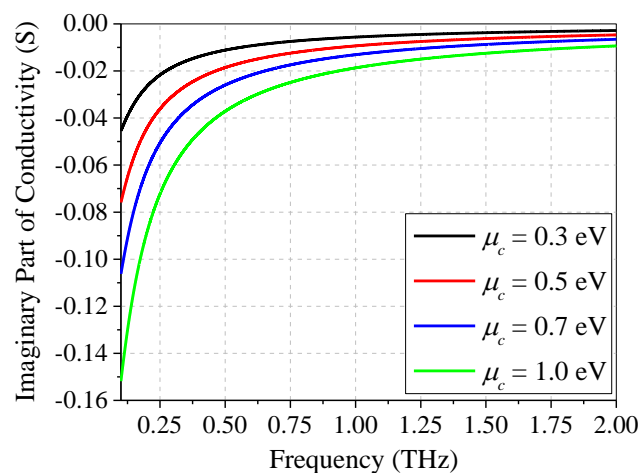
$$\sigma_g\left(\omega,\mu_c,\Gamma,T\right) = -i\frac{e^2 k_B T}{\pi\hbar^2\left(\omega-2i\Gamma\right)}\left[\frac{\mu_c}{k_B T} + 2\ln\left(e^{-\frac{\mu_c}{k_B T}} + 1\right)\right] \tag{1}$$

where ω is the angular frequency, e is the charge of electron, k_B is the Boltzmann constant, T is the temperature (300 K), $\hbar$ is the reduced Planck constant, Γ is the scattering rate (0.1 meV), and μ_c is the chemical potential.

In Fig. 2, it is shown the variation of real and imaginary parts of graphene conductivity with frequency for different values of the chemical potential. As one can see, its imaginary part is negative, which in turn is the necessary condition for graphene based devices to support transverse magnetic (TM) surface plasmon polariton (SPP) waves [12].

(a)

(b)

Fig. 2.Surface conductivity of graphene as a function of frequency for different values of the chemical potential: (a) real part and (b) imaginary part.

III.   ANALYTICAL FORMULAS FOR THE CALCULATION OF THE FREQUENCY RESPONSE

An analytical description of the presented component based on the TCMT has been developed. By using the formalism presented in [13], the TCMT based equations that describe the evolution of the electromagnetic field in the system comprising the two disk resonators can be written as follows:

$$\frac{da_1}{dt} = \left(i\omega_1 - \frac{1}{\tau_{i,1}} - \frac{1}{\tau_{w,1}} \right) a_1 + \sqrt{\frac{1}{\tau_{w,1}}} s_i - i\mu a_2 \tag{2}$$

$$\frac{da_2}{dt} = \left(i\omega_2 - \frac{1}{\tau_{i,2}} - \frac{1}{\tau_{w,2}} \right) a_2 + \sqrt{\frac{1}{\tau_{w,2}}} s_i - i\mu a_1 \tag{3}$$

$$s_t = s_i - \sqrt{\frac{1}{\tau_{w,1}}} a_1 - \sqrt{\frac{1}{\tau_{w,2}}} a_2 \tag{4}$$

$$s_r = -\sqrt{\frac{1}{\tau_{w,1}}} a_1 - \sqrt{\frac{1}{\tau_{w,2}}} a_2 \tag{5}$$

where a_n is the amplitude of the resonant mode in the nth disk ($n = 1, 2$), ω_n is the resonant frequency of the mode in the nth disk $\tau_{i,n}$ is the decay rate of the mode in the nth disk due to intrinsic losses, $\tau_{w,n}$ is the decay rate of the mode in the nth disk to the input/output, μ is the mutual coupling coefficient between the two modes, s_i is the amplitude of the incident wave, s_r is the amplitude of the reflected wave,and s_t is the amplitude of the transmitted wave.

From this set of equations, one can define the formulas for the transmission and reflection coefficients of the array with double disk resonators as follows:

$$t(\omega) = \frac{s_t}{s_i} = 1 - \sqrt{\frac{1}{\tau_{w,1}}} \frac{A_1}{B_1} - \sqrt{\frac{1}{\tau_{w,2}}} \frac{A_2}{B_2} \tag{6}$$

$$r(\omega) = \frac{s_r}{s_i} = -\sqrt{\frac{1}{\tau_{w,1}}} \frac{A_1}{B_1} - \sqrt{\frac{1}{\tau_{w,2}}} \frac{A_2}{B_2} \tag{7}$$

with

$$A_1 = \sqrt{\frac{1}{\tau_{w,1}}} - \frac{i\mu\sqrt{\frac{1}{\tau_{w,2}}}}{i(\omega-\omega_2)+\frac{1}{\tau_{i,2}}+\frac{1}{\tau_{w,2}}} \tag{8}$$

$$B_1 = i(\omega-\omega_1)+\frac{1}{\tau_{i,1}}+\frac{1}{\tau_{w,1}}+\frac{\mu^2}{i(\omega-\omega_2)+\frac{1}{\tau_{i,2}}+\frac{1}{\tau_{w,2}}} \tag{9}$$

$$A_2 = \sqrt{\frac{1}{\tau_{w,2}}} - \frac{i\mu\sqrt{\frac{1}{\tau_{w,1}}}}{i(\omega-\omega_1)+\frac{1}{\tau_{i,1}}+\frac{1}{\tau_{w,1}}} \tag{10}$$

$$B_2 = i(\omega - \omega_2) + \frac{1}{\tau_{i,2}} + \frac{1}{\tau_{w,2}} + \frac{\mu^2}{i(\omega - \omega_1) + \frac{1}{\tau_{i,1}} + \frac{1}{\tau_{w,1}}} \qquad (11)$$

Regarding transmittance (T) and reflectance (R) of the structure, they can be defined as follows:

$$T(\omega) = |t(\omega)|^2 \qquad (12)$$

$$R(\omega) = |r(\omega)|^2 \qquad (13)$$

IV.   RESULTS AND DISCUSSIONS

In order to test our analytical model, we have performed computational simulations of the proposed component with the software product ANSYS HFSS, which in turn is based on the finite element method. We have considered only normal incidence (see Fig. 1) and the performance characteristics of the device are not dependent on the polarization state of the feeding.

In Figs. 3 and 4, it can be observed that, regarding the transmission and reflection spectra, the computational results are in good agreement with those provided by the presented TCMT-based approach, both for the case with graphene disks suspended in air (Fig. 3) and for the case with the dielectric substrate between the two disks (Fig. 4).
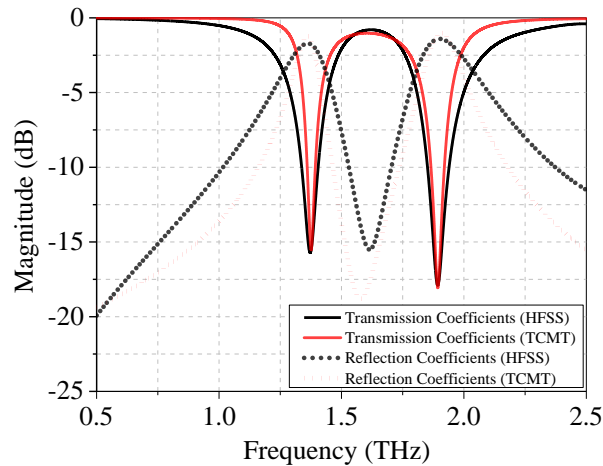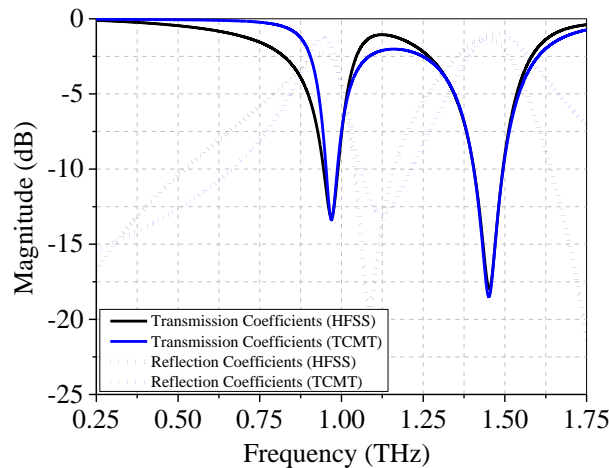

Fig. 3.Computational and analytical results for the double disk resonator without dielectric substrate. The values of the TCMT parameters are: f_1 = 1.89 THz, $\tau_{w,1}$= 2 ps, $\tau_{i,1}$ = 21 ps, f_2 = 1.38 THz, $\tau_{w,2}$ = 4 ps, $\tau_{i,2}$ = 12 ps, and $\mu = 1 \times 10^{11}$ s^{-1}.

Fig. 4.Computational and analytical results for the double disk resonator with dielectric substrate. The values of the TCMT parameters are: f_1 = 1.45 THz, $\tau_{w,1}$ = 1.2 ps; $\tau_{i,1}$ = 20 ps, f_2 = 0.96 THz, $\tau_{w,2}$ = 4 ps, $\tau_{i,2}$ = 6.6 ps, and $\mu = 2 \times 10^{11}$ s^{-1}.

Besides, from Figs. 3 and 4 it is possible to verify that the dielectric substrate cause a significant red-shift of the resonant frequency for both disks. Such as in [14], [15], the increase in the average refractive index of the whole structure caused by the substrate is related to the lower resonant frequencies observed in Fig. 4.

A. *Influence of the TCMT parameter μ for the case without dielectric substrate*

The frequency response of the structure, considering the parameter h equal to 0.1, 10 and 30 μm, is shown in Fig. 5. One can see that it is highly dependent on the coupling between the two resonator disks. We have noticed that, by increasing the parameter h from 10 μm to 30 μm, there is a decrease in the maximum transmission levels and width of the window of plasmonically induced transparency (related to the Fano resonance effect), mostly because of the decrease on the coupling between both disks. For these two values of h, the transmission spectrum has two minimum points corresponding to the resonant frequencies of the two disks that also vary with this coupling. However, when the parameter is very small (0.1 μm), one can see that the frequency response of the device shows only one minimum point. We believe that, in the latter case, the coupling of the disks is very strong because they are quite close, so that they can be regarded as only one disk, that is, there is only one resonant frequency in the coupled system.
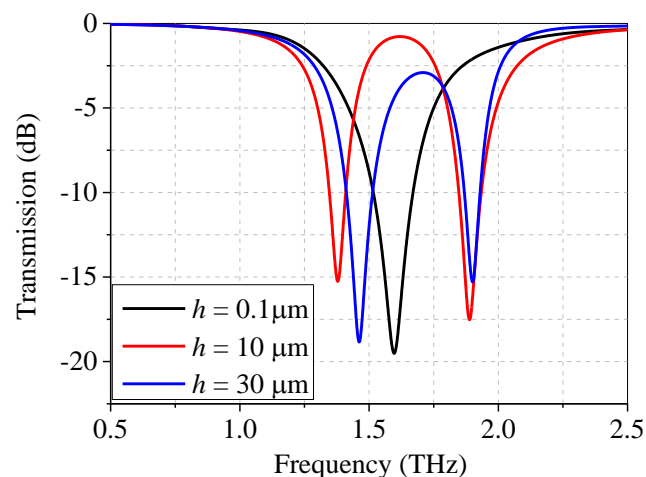

Fig. 5. Transmission spectra for h = 0.1, 10, and 30 μm (without dielectric substrate).

We have also calculated, for the considered values of the parameter h, the E_z field component at the resonant frequency 1.6 THz for both disks (see Fig. 6) and for all the considered values of h. Again, one can observe that the parameter h directly influences the coupling force between the disks, which in turn influences the maximum and minimum transmission levels at the resonant frequencies of the structure.
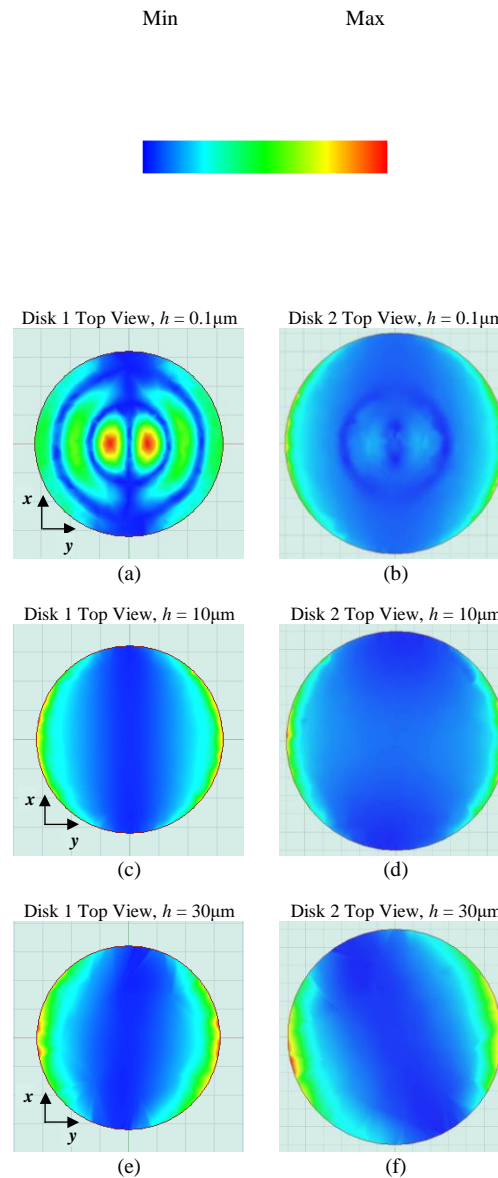
Fig. 6. Distribution of the electric field component E_z on the two disks at the resonant frequency 1.6 THz, for $h = 0.1$, 10, and 30 μm (without dielectric substrate).

In order to relate the computational results concerning the variation of the parameter h (or, equivalently, the coupling between both disks) to the analytical TCMT approach, we have calculated the transmission coefficient as a function of the parameter μ (see Fig. 7) by using formula (12).

One can see that, the higher the parameter μ, the higher the transmission levels at the Fano resonance frequency and the higher the frequency shift of the two resonances induced by the mutual coupling. By comparing Figs. 5 and 7, it is possible to state that this is equivalent to decreasing parameter h. Therefore, the geometrical parameter h is closely related to the analytical parameter μ included in the presented TCMT based description.
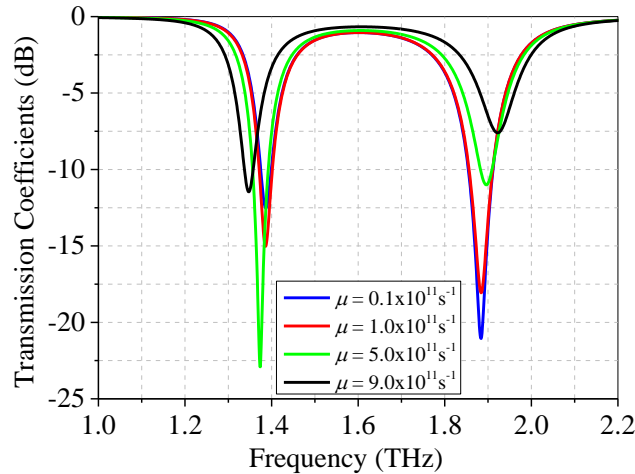
Fig. 7.Transmission coefficients as a function of parameter μ.

B. Influence of the TCMT parameter μ for the case with dielectric substrate

The same analysis has been performed for the case including the dielectric substrate between both disks. In Fig. 8, the resonant frequencies for the two coupled disks as a function of the dielectric thickness h are displayed. We have found that, due to the dielectric substrate in the structure, the resonant frequencies are shifted to smaller values when compared to those presented in Fig. 5.

Similarly to the case without the dielectric substrate, one can see that the higher the parameter h (considering the cases with $h = 10$ μm and $h = 20$ μm), the lower the transmission levels and the lower the width of the PIT region. Besides, for the maximum coupling case ($h = 0.1$ μm), it can be verified that the two resonant frequencies turn into only one (see Fig. 8), as previously seen in section IV.A.

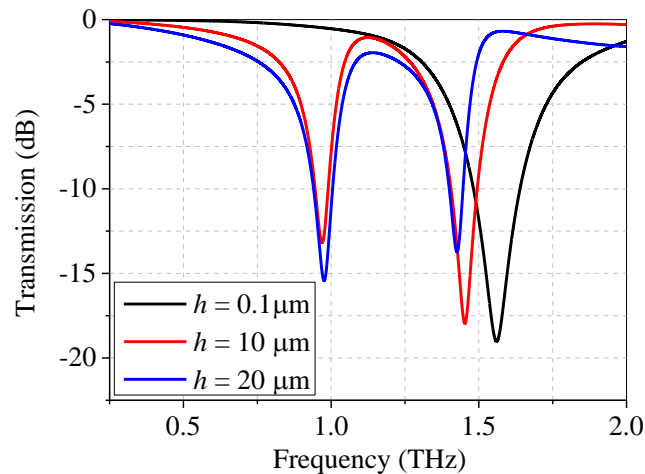Fig. 8. Transmission spectra for $h = 0.1$, 10, and 20 μm (with dielectric substrate).

For a better understanding of the relationship between the parameter h and the mutual coupling, we show in Fig. 9 the distribution of the electric field component E_z in the graphene disks at the resonant frequency 1.54 THz.
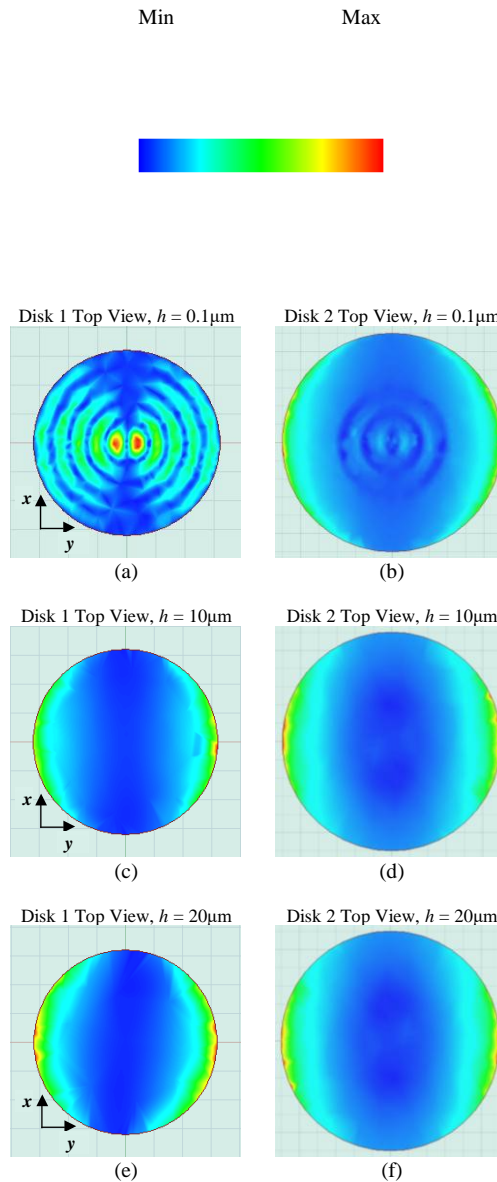
Fig. 9. Distribution of the electric field component E_z on the two disks at the resonance frequency 1.54 THz, for $\varepsilon_r = 3.75$ and $h = 0.1$, 10, and 20 μm (with dielectric substrate).

In Fig. 10, it is shown the influence of the TCMT parameter μ in the frequency response of the component. One can see again that the geometrical parameter h can be associated to the TCMT parameter μ, that is, it is possible to change the characteristics of the PIT region by modifying the value of μ.
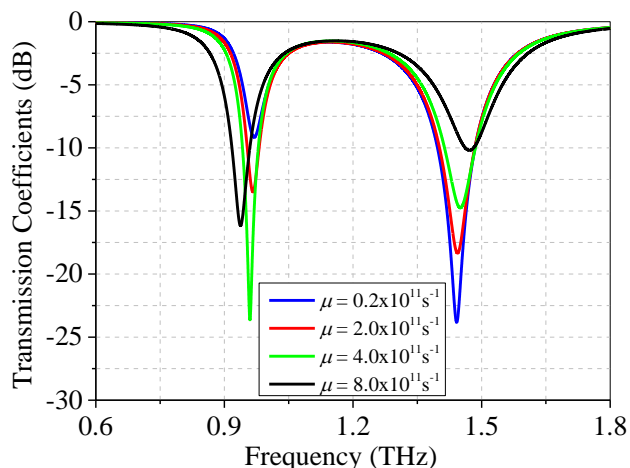
Fig. 10.Frequency response as a function of parameter μ.

C. *Variation of the graphene chemical potential*

We have also studied the influence of the chemical potential (μ_c) on the frequency response of the component. Fig. 11 shows the transmission curves for different values of the graphene chemical potential for the case with dielectric substrate. The typical value $\mu_c = 0.5$ eV [16], [17] has been considered in the calculation of the transmission spectra presented in Figs. 3, 4, 5, and 8. One can verify that as the chemical potential gets higher, the resonant frequencies of both graphene disks are blue-shifted and the transmission levels at the resonant frequencies are decreased. These results show that, by changing the chemical potential, it is possible to shift the transparency window of the structure and use it as a frequency-tunable electromagnetic filter. Besides, this feature enables one the use of the proposed structure as a switch for THz applications.
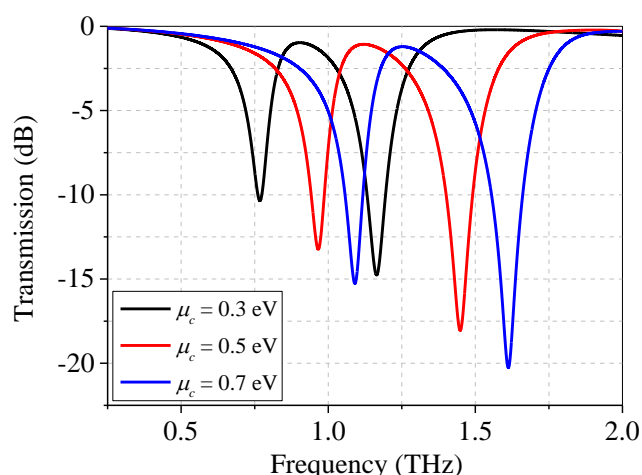

Fig. 11. Frequency response for different values of chemical potential (μ_c).

V.   CONCLUSIONS

We have suggested a new graphene-based structure that can be used as a frequency-tunable filter or as an electromagnetic switch in the THz frequency band. Also, a TCMT-based approach for the analysis and design of the proposed device has been developed andthe analytical results provided by the TCMT equations are in a good agreement with those obtained from full-wave numerical

computations. By relating the analytical parameters of the TCMT description to the geometrical/material parameters of the graphene-based double disk system, we have shown how to use the analytical model in the analysis and design of the structure.

<div align="center">APPENDIX</div>

A. Calculation of disk diameters

The diameters (*D*) of both graphene disks can be approximately defined by considering that, for the dipole TM mode, the following relationship remains valid: $\pi D = \lambda_{spp}$, where λ_{spp} is the wavelength of the SPP mode. Taking into account that $\lambda_{spp} = 2\pi/\text{Re}(k_{spp})$, where k_{spp} is the wavevector of the plasmonic waves, one can calculate the diameter *D* by using the following formula:

$$D = \frac{2}{\text{Re}(k_{spp})} \tag{14}$$

For the general case of an infinite graphene layer sandwiched between two dielectric media, the value of k_{spp} can be calculated by using the following formula [18]:

$$k_{spp} = \frac{\pi \hbar^2 \varepsilon_0 (\varepsilon_{r1} + \varepsilon_{r2})}{e^2 \mu_c}\left(1 + \frac{i}{\tau\omega}\right)\omega^2 \tag{15}$$

Where ε_0 is the electrical permittivity of free space, ε_{r1} and ε_{r2} are the relative permittivities of the two dielectric materials, and $\tau = 1/\Gamma$ is the relaxation time of graphene.

By substituting Eq. (15) into Eq. (14), we have calculated approximate values for the diameters of both graphene disks for specific resonant frequencies. In order to check the validity of this method, we have also numerically calculated the resonant frequency of some graphene disks, with different diameters, by using the software product ANSYS HFSS (see Fig. 12). One can see that there is a good agreement between the results provided by (14)-(15) and those obtained from the computational simulations, with a 4.31% mean error.
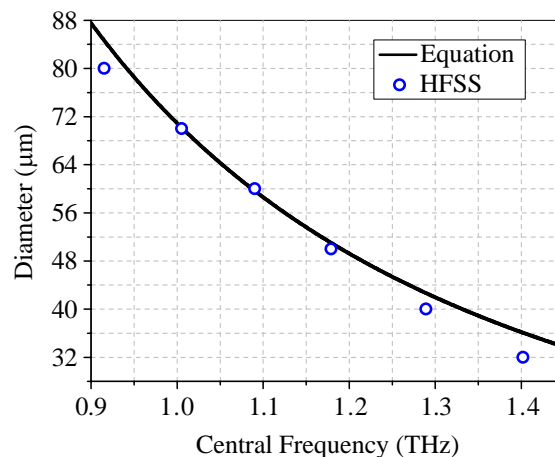

Fig. 12.Relationship between diameter and resonant frequency for graphene-based disk resonators.

REFERENCES

[1] M. Tonouchi, "Cutting-edge terahertz technology," *Nature Photonics*, vol. 1, no. 2, pp. 97-105, 2007.
[2] W. Min, H. Sun, Q. Zhang, H. Ding, W. Shen, and X. Sun, "A novel dual-band terahertz metamaterial modulator," *Journal of Optics*, vol. 18, no. 6, pp. 065103, 2016.
[3] C. Lee, X. Wei, J.W. Kysar, and J. Hone, "Measurement of the elastic properties and intrinsic strength of monolayer graphene," *Science*, vol. 321, no. 5887, pp. 385-388, 2008.
[4] C. Liu, P. Liu, C. Yang, and L. Bian, "Terahertz metamaterial based on dual-band graphene ring resonator for modulating and sensing applications," *Journal of Optics*, vol. 19, no. 11, pp. 115102, 2017.
[5] H. Cheng, S.Chen, P.Yu, X.Duan, B.Xie, and J.Tian, "Dynamically tunable plasmonically induced transparency in periodically patterned graphene nanostrips," *Applied Physics Letters*, vol. 103, no. 20, pp. 203112, 2013.
[6] V. Dmitriev and C. Nascimento, "Planar THz electromagnetic graphene pass-band filter with low polarization and angle of incidence dependencies," *Applied Optics*, vol. 54, no. 6, pp. 1515-1520, 2015.
[7] B. Zhan, C. Li, J. Yang, G. Jenkins, W. Huang, andX. Dong,"Graphene Field-Effect Transistor and Its Application for Electronic Sensing,"*Small*, vol. 10, no. 20, pp. 4042-4065, 2014.
[8] S. Cakmakyapan, P.K. Lu, A. Navabi, and M. Jarrahi, "Gold-patched graphene nano-stripes for high-responsivity and ultrafast photodetection from the visible to infrared regime,"*Light: Science & Applications*, vol. 7, no. 1, p. 20,2018.
[9] L. Huang, S. Wu, Y. Wang, X. Ma, H. Deng, S. Wang, Y. Lu, C. Li, and T. Li, "Tunable unidirectional surface plasmonpolariton launcher utilizing a graphene-based single asymmetric nanoantenna," *Optical Materials Express*, vol.7, no. 2, pp. 569-576, 2017.
[10] H. A. Haus andW. Huang, "Coupled-mode theory," *Proceedings of the IEEE*, vol. 79, no. 10, pp. 1505-1518, 1991.
[11] G. W. Hanson, "Dyadic Green's functions and guided surface waves for a surface conductivity model of graphene,"*Journal of Applied Physics*, vol. 103, no. 6, pp. 64302-64309, 2008.
[12] W. Gao, G. Shi, Z. Jin, J. Shu, Q. Zhang, R. Vajtai, P. M. Ajayan, J. Kono, and Q. Xu, "Excitation and active control of propagating surface plasmon polaritons in graphene," *Nano Letters*, vol. 13, no. 8, pp. 3698-3702, 2013.
[13] Q. Li, T. Wang, Y. Su, M. Yan, and M. Qiu, "Coupled mode theory analysis of mode-splitting in coupled cavity system,"*Optics Express*, vol. 18, no. 8, pp. 8367-8382, 2010.
[14] A. Akhavan, H. G. Fard, and V. Varmazyari, "Dynamically-Tunable Terahertz Band-Stop Filter Based on Multilayer Graphene Metamaterial," *International Journal of Optics and Applications*, vol. 7, no.1, pp. 7-12, 2017.
[15] T. Kim, W. S. Lee, S. M. Kang, N. C. Park, K. S. Park, and Y. P. Park, "Effects of dielectric substrate properties for optical phenomena in a nanoscale ridge aperture," *Journal of Optics*, vol. 14, no. 4, pp. 045001, 2012.
[16] X. He, Q. Zhang, G. Lu, G. Ying, F. Wu, and J. Jiang, "Tunable ultrasensitive terahertz sensor based on complementary graphene metamaterials," *Rsc Advances*, vol. 6, no. 57, pp. 52212-52218, 2016.
[17] W. Wang, Z. Meng, R. Liang, S. Chen, L. Ding, F. Wang, L. Hongzhan, M. Hongyun, and Z. Wei,"A dynamically tunable plasmonic multi-functional device based on graphene nano-sheet pair arrays," *Optics Communications*, vol. 415,pp. 130-134, 2018.
[18] M. Jablan, H. Buljan, and M. Soljačić, "Plasmonics in graphene at infrared frequencies,"*Physical Review B*, vol. 80, no. 24, pp. 245435, 2009.